J Mater Sci (2009) 44:2444–2453
DOI 10.1007/s10853-009-3309-y

The inhibition of mild steel corrosion in hydrochloric acid media by two Schiff base compounds

M. Behpour · S. M. Ghoreishi · A. Gandomi-Niasar · N. Soltani · M. Salavati-Niasari

Received: 23 August 2008 / Accepted: 2 February 2009 / Published online: 5 March 2009

Abstract Schiff bases of 2-({-1-methyl-3-[(2-sulfanylphenyl)imino]butylidene}-amino)-1-benzenethiol and 2-({-1,2-diphenyl-2-[(2-sulfanylphenyl)imino]ethylidene}amino)-1-benzenthiol are investigated as corrosion inhibitors in acid solution. Polarization, electrochemical impedance spectroscopy, and weight loss measurements were performed on mild steel in 15% HCl with and without the inhibitors. A significant decrease in the corrosion rate of mild steel was observed in the presence of investigated inhibitors. Polarization curves indicate that both compounds are mixed inhibitors, affecting both cathodic and anodic corrosion currents. The adsorption of inhibitors on mild steel surface in 15% HCl was found to follow Langmuir adsorption isotherm. Thermodynamic adsorption parameters (K_{ads}, ΔG_{ads}) of studied Schiff bases were calculated using the Langmuir adsorption isotherm. Activation parameters of the corrosion process such as activation energies, E_a, activation enthalpies, ΔH^*, and activation entropies, ΔS^*, were calculated by the obtained corrosion currents at different temperatures.

Introduction

Since corrosion and abrasion are the effective factors in the degradation of industrial parts, many attempts have been made to find methods of reducing corrosion and wear costs [1–7]. One of the most important methods in the corrosion protection of metals is using inhibitors. Inhibitors are widely used for protection against corrosion in different environment [8–13]. The choice of inhibitor is based on two considerations: first it could be synthesized conveniently from relatively cheap raw materials; secondly, it contains the electron cloud on the aromatic ring or electronegative atoms such as nitrogen, oxygen in the relatively long-chain compounds. The presence of hetero atoms such as oxygen, nitrogen, sulfur, phosphorus, triple bonds, and aromatic rings in the inhibitors chemical structure enhance the adsorption process. It has been reported that the inhibition efficiency (IE) (%) of heterocyclic organic compounds follows the sequence: O < N < S < P [14, 15]. Organic molecules of this type adsorb on the metal surface and form a bond between the heteroatom pair and/or the π electron cloud and the metal, thereby reducing the corrosion in acidic solutions [16, 17]. Some Schiff bases have been reported earlier as corrosion inhibitors for copper [18–20], aluminum [21], zinc [22], and iron [23]. Many organic molecules are used to inhibit mild steel corrosion [24, 25]. Several Schiff bases have also been investigated as corrosion inhibitors for mild steel in acidic media [26–28].

The objective of this study is to study the inhibitory effect of two Schiff bases on the corrosion inhibition of mild steel in 15% HCl solution. The behavior of mild steel in 15% HCl with and without inhibitor is studied using gravimetric, polarization, and electrochemical impedance spectroscopy (EIS) measurements.

Experimental

Materials

The Schiff bases were synthesized in the laboratory following a procedure reported previously [29]. The molecular structures of the Schiff bases are shown in Fig. 1.

M. Behpour (✉) · S. M. Ghoreishi · A. Gandomi-Niasar · N. Soltani · M. Salavati-Niasari
Department of Chemistry, Faculty of Science, University of Kashan, Kashan, Islamic Republic of Iran
e-mail: m.behpour@kashanu.ac.ir

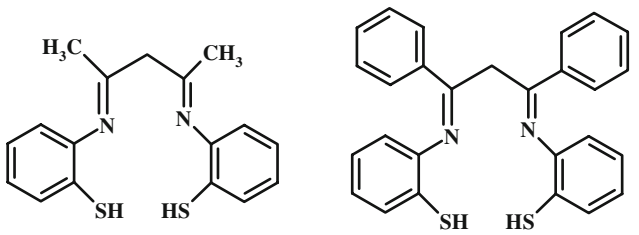

Compound 1 Compound 2

Fig. 1 Structures of the studied Schiff bases

Table 1 Chemical composition of steel specimens obtained from quantometric method

C	0.52
Si	0.0027
Mn	0.23
P	0.006
S	0.010
Cr	0.012
Ni	0.04
Al	0.056
Cu	0.067
Nb	0.0032
Ti	0.0021
V	0.0015
Fe	99.0495

The chemical composition (wt%) of the steel specimen (determined by SPECTROLAB quantometer) is given in Table 1.

Square specimens with dimensions 1 cm × 1 cm × 0.2 cm were used for weight loss measurements. For polarization studies, the steel specimen was embedded in PVC holder using epoxy resin with an exposed area of 1 cm^2 as a working electrode. The specimens were polished with emery paper no. 400-1200 grade. They were cleaned with acetone, washed with double-distilled water, and finally dried at room temperature before being immersed in the acid solution. The acid solutions (15%) were made from analytical grade 37% HCl and double-distilled water. The concentration range of inhibitor employed was 5×10^{-6} to 1×10^{-3} M in 15% HCl.

Weight loss measurement

The weight loss experiments were carried out in a glass vessel containing 50 mL of 15% HCl with and without the addition of different concentrations (5×10^{-6} to 1×10^{-3}) of Schiff bases at 25 °C. Mild steel specimens were immersed in the test acid solutions for 6 h. The temperature was controlled by an aqueous thermostat bath. After the required immersion time, the specimens were withdrawn, rinsed with doubly-distilled water, ethanol, and finally dried at room temperature. Then, the loss in weight was determined by analytic balance. The experiments were done in triplicate and the average value of the weight loss was considered. Corrosion rates were calculated from the weight loss of the specimens according to Eq. 1.

$$W = \frac{m_1 - m_2}{At}, \tag{1}$$

where m_1 and m_2 are the weight loses (mg) before and after immersion in the test solutions, A is the area of the specimens (cm^2), and t is the exposure time (h). The IE and the degree of surface coverage (Θ) were calculated using the following equations:

$$\mathrm{IE}\% = \left(\frac{W - W'}{W}\right) \times 100, \tag{2}$$

$$\theta = \frac{W - W'}{W}, \tag{3}$$

where W, W' are the uninhibited and inhibited corrosion rates (in terms of mg cm^{-2} h^{-1}), respectively.

Potentiodynamic polarization measurement

Electrochemical experiments were performed in a conventional three electrodes electrochemical cell with a platinum counter electrode and silver–silver chloride ($Ag/AgCl/Cl^-$) electrode as reference electrode. The polarization curves are recorded with an Autolab potentiostate-galvanostate model PGSTAT 35. Before recording the polarization curves, working electrode is first immersed into the test solution for 30 min in order to attain its free corrosion potential. Scan rate of potential was 0.5 mV s^{-1} and potential was scanned in the range of −500 to +500 mV relative to the corrosion potential. Polarization data were analyzed using GPES electrochemical software and corrosion current density values were obtained by Tafel extrapolation method. The temperature was adjusted to 35–65 °C using TAMSON model T1000 thermostat.

The polarization curves were carried out in the absence and presence of different concentrations of inhibitors.

The IE (%) was calculated from:

$$\mathrm{IE}\% = \left(\frac{I_{\mathrm{corr}} - I'_{\mathrm{corr}}}{I_{\mathrm{corr}}}\right) \times 100, \tag{4}$$

where I_{corr} and I'_{corr} are the uninhibited and inhibited corrosion current densities, respectively.

Electrochemical impedance spectroscopy

EIS measurements were carried out at the open circuit potential (E_{ocp}), using a computer-controlled potentiostat (Autolab). Impedance data were analyzed using a Pentium IV computer and FRA software.

Impedance spectra were obtained in the frequency range of 100 kHz to 10 MHz after 30 min of immersion in non-de-aerated solutions. A sine wave with 5 mV amplitude was used to perturb the system.

Surface analysis

The surface morphology of the mild steel samples after immersion in HCl solution with and without inhibitor, coated by a film of 50 nm of gold by sputtering, was investigated by scanning electron micrograph (SEM) using a PHILIPS model XL30 microscope.

Results and discussion

Weight loss tests

Table 2 shows the values of inhibition efficiencies and corrosion rates obtained from weight loss method at different concentrations of inhibitors in 15% HCl at room temperature. The results show that the IE increases and the corrosion rate decreases with increase in inhibitor concentration. The IE data showed that compound 2 has greater interaction with mild steel compared to compound 1. However, the difference between efficiencies was low and indicated that both compounds exhibit good effectiveness. The maximum IE (98%) was obtained with compound 2 at a concentration of 1×10^{-3} M.

Table 2 Corrosion parameters for mild steel in 15% HCl in the presence and absence of different concentrations of Schiff bases obtained from weight loss

Inhibitors	Concentration (M)	Corrosion rate (mg cm^{-2} h^{-1})	Surface coverage (θ)	IE (%)
Blank	–	11.61	–	–
Compound 1	5×10^{-6}	11.73	–	–
	1×10^{-5}	3.09	0.734	73.4
	5×10^{-5}	1.599	0.862	86.2
	1×10^{-4}	1.18	0.89	89.0
	5×10^{-4}	0.64	0.94	94.0
	1×10^{-3}	0.474	0.96	96.0
Compound 2	5×10^{-6}	1.58	0.86	86.0
	1×10^{-5}	1.21	0.89	89.0
	5×10^{-5}	0.93	0.92	92.0
	1×10^{-4}	0.68	0.94	94.0
	5×10^{-4}	0.49	0.96	96.0
	1×10^{-3}	0.22	0.98	98.0

Tafel polarization measurements

Figures 2 and 3 show potentiodynamic curves for the mild steel electrode in 15% HCl solution with and without different concentrations of inhibitors 1 and 2. It is clear that the current density decreases with the presence of Schiff bases; this indicates that these compounds are adsorbed on the metal surface and hence inhibition occurs. Values of corrosion potential (E_{corr}), corrosion current density (I_{corr}),

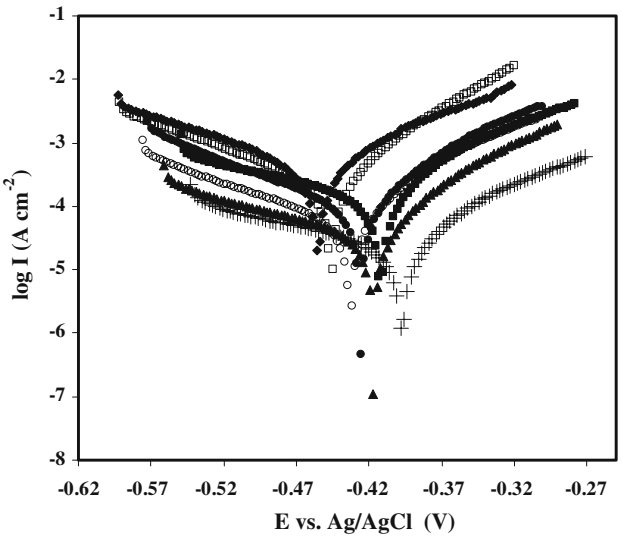

Fig. 2 Potentiodynamic polarization curves of mild steel in 15% HCl containing different concentration of Schiff base 1 (15% HCl (*open square*), 5×10^{-6} M (*filled diamond*), 1×10^{-5} M (*open circle*), 5×10^{-5} M (*filled square*), 1×10^{-4} M (*filled circle*), 5×10^{-4} M (*filled triangle*), 1×10^{-3} M (*plus*))

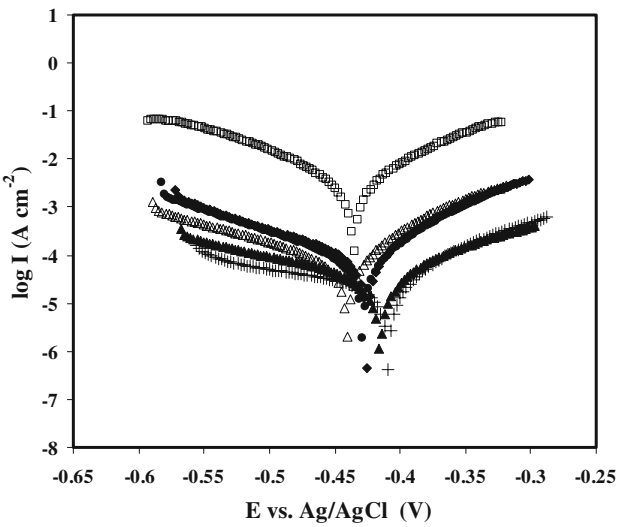

Fig. 3 Potentiodynamic polarization curves of mild steel in 15% HCl containing different concentration of Schiff base 2 (15% HCl (*open square*), 5×10^{-6} M (*filled diamond*), 1×10^{-5} M (*open circle*), 5×10^{-5} M (*filled square*), 1×10^{-4} M (*filled circle*), 5×10^{-4} M (*filled triangle*), 1×10^{-3} M (*plus*))

Table 3 Electrochemical polarization parameters for the mild steel in 15% HCl containing different concentrations of Schiff bases

Inhibitor	Concentration (M)	$-E_{corr}$ (mV)	I_{corr} (μA cm^{-2})	$-b_c$ (mV dec^{-1})	b_a (mV dec^{-1})	IE (%)
Blank		435	3061.5	90	75	–
Compound 1	5×10^{-6}	443	3031.5	96	88	–
	1×10^{-5}	431	759.13	217	95	75.2
	5×10^{-5}	412	416.30	207	82	86.4
	1×10^{-4}	430	315.28	183	69	89.7
	5×10^{-4}	417	159.17	263	64	94.8
	1×10^{-3}	397	125.50	214	81	95.9
Compound 2	5×10^{-6}	426	370.38	200	73	87.9
	1×10^{-5}	433	284.67	217	77	90.7
	5×10^{-5}	441	221.00	207	68	92.7
	1×10^{-4}	407	212.74	233	95	93.1
	5×10^{-4}	428	101.93	119	62	96.6
	1×10^{-3}	415	45.91	210	97	98.5

obtained by extrapolation of the Tafel lines, cathodic, and anodic Tafel slope (b_c, b_a), and corrosion IE (%) for different concentrations of inhibitors 1 and 2 in 15% HCl are given in Table 3.

The potentiodynamic curves show that there is a clear reduction of both the anodic and cathodic currents in the presence of inhibitors 1 and 2 compared with those for the blank solution. It is clear that the cathodic reaction (hydrogen evolution) and the anodic reaction (dissolution metal) were inhibited. The values of cathodic Tafel slope (b_c) for two Schiff bases are found to increase in the presence of inhibitor. The Tafel slope variations suggest that both Schiff bases influence the kinetics of the hydrogen evolution reaction [30]. This indicates an increase in the energy barrier for proton discharge, leading to less gas evolution [31]. The approximately constant values of anodic Tafel slope (b_a) for Schiff bases 1 and 2 indicate that these compounds were first adsorbed onto the metal surface and impeded by merely blocking the reaction sites of the metal surface without affecting the anodic reaction mechanism [32].

It can be seen from Table 3 that the corrosion potentials of inhibitors 1 and 2 shift in the positive direction. The shift of the corrosion potential in the positive sense as compared to the uninhibited situations shows that the effect on the anodic branch and reaction is somewhat more pronounced than on the cathodic reaction.

The compounds tested as corrosion inhibition of mild steel in 15% HCl are effective even with small concentrations. The higher values of IE indicate the higher surface coverage, due to the inhibitors adsorption on the metal surface.

Electrochemical impedance spectroscopy

The corrosion of mild steel in 15% HCl solution in the presence of the Schiff base compounds was investigated by the EIS method at 25 °C after 30 min immersion. Nyquist plots in the absence and presence of the Schiff base compounds are presented in Figs. 4 and 5.

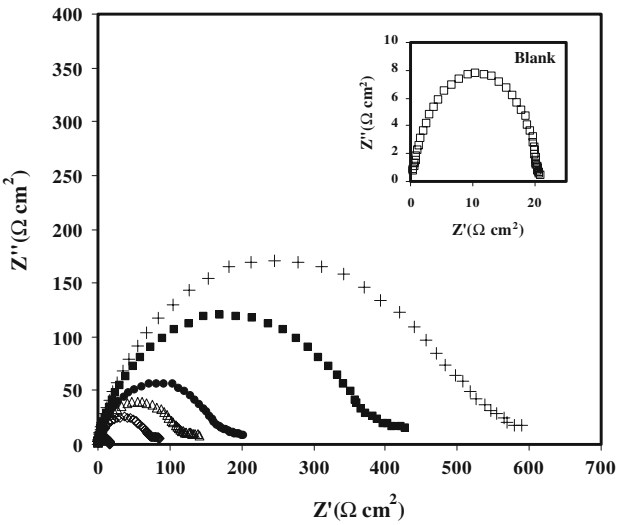

Fig. 4 Nyquist plots for the mild steel in 15% HCl in the presence of different concentrations of Schiff base 1 (15% HCl (*open square*), 5×10^{-6} M (*filled diamond*), 1×10^{-5} M (*open circle*), 5×10^{-5} M (*filled square*), 1×10^{-4} M (*filled circle*), 5×10^{-4} M (*filled triangle*), 1×10^{-3} M (*plus*))

It is apparent that all Nyquist plots show a single capacitive loop, both in uninhibited and inhibited solutions. The impedance data of mild steel in 15% HCl are analyzed using the circuit shown in Fig. 6, in which R_s represents the electrolyte resistance, R_t the charge transfer resistance. One constant phase element (Q_{dl}) is substituted for the capacitive element to give a more accurate fit, as most capacitive loops are depressed semicircles rather than regular semicircles [33].

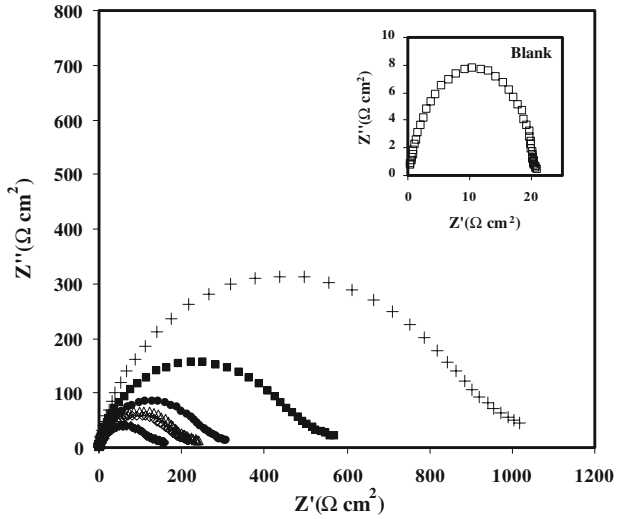

Fig. 5 Nyquist plots for the mild steel in 15% HCl in the presence of different concentrations of Schiff base 2 (15% HCl (*open square*), 5×10^{-6} M (*filled diamond*), 1×10^{-5} M (*open circle*), 5×10^{-5} M (*filled square*), 1×10^{-4} M (*filled circle*), 5×10^{-4} M (*filled triangle*), 1×10^{-3} M (*plus*))

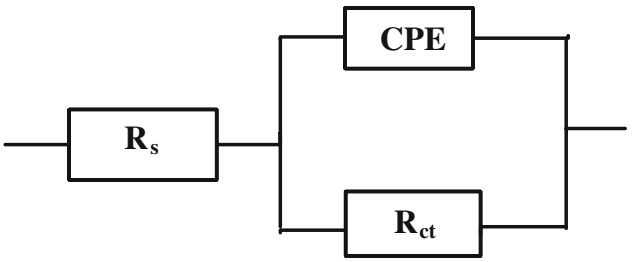

Fig. 6 Electrochemical equivalent circuit diagram for metal–electrolyte interface

The impedance of a constant phase element is described by the expression:

$$Z_Q = Y_0^{-1}(j\omega)^{-n}, \tag{5}$$

where Y_0 is a proportional factor, n has the meaning of a phase shift. According to Hsu and Mansfeld [34], the values of the double layer capacitance (C_{dl}) can be obtained from the equation:

$$C_{dl} = Y_0\left(\omega''_m\right)^{n-1}, \tag{6}$$

where ω''_m is the frequency at which the imaginary part of the impedance has a maximum. Values of elements fitted and that of C_{dl} calculated are listed in Table 4. In the case of impedance studies, IE (%) is calculated from the equation:

$$E\% = \frac{R'_t - R_t}{R'_t} \times 100, \tag{7}$$

where R_t and R'_t are the values of the charge transfer resistance without and with inhibitor, respectively.

As it can be seen from Table 4, the R_t values increased with the increasing concentrations of the inhibitors. On the other hand, the values of C_{dl} decreased with an increase in the inhibitors concentration thus with inhibition efficiencies. This situation was the result of an increase in the surface coverage by the inhibitor, which led to an increase in the IE The decrease in the C_{dl}, which can result from a decrease in local dielectric constant and/or an increase in the thickness of the electrical double layer, suggested that the Schiff base molecules function by adsorption at the metal/solution interface. Thus, the change in C_{dl} values was caused by the gradual displacement of water molecules

Table 4 Electrochemical parameters of impedance for mild steel in 15% HCl without and with addition of various concentrations of studied Schiff bases

Inhibitor	Concentration (M)	R_s (Ω)	R_{ct} (Ω)	Q		C_{dl} (μF cm^{-2})	IE (%)
				Y_0 (μF cm^{-2})	n		
Blank		0.22	17.7	273.64	0.76	215.7	–
Compound 1	5×10^{-6}	0.21	17.3	268.43	0.78	209.4	–
	1×10^{-5}	0.23	76.0	21.45	0.86	45.7	76.71
	5×10^{-5}	0.21	121.3	6.31	0.85	18.3	85.40
	1×10^{-4}	0.23	178.3	6.15	0.89	8.8	90.07
	5×10^{-4}	0.22	376.0	5.91	0.90	6.9	95.29
	1×10^{-3}	0.31	522.0	5.34	0.92	6.4	96.60
Compound 2	5×10^{-6}	0.49	137.6	6.2	0.88	15.7	87.13
	1×10^{-5}	0.44	201.1	5.9	0.89	7.9	91.19
	5×10^{-5}	0.42	214.4	5.3	0.90	7.5	91.47
	1×10^{-4}	0.13	269.8	5.2	0.91	6.8	93.43
	5×10^{-4}	0.16	487.0	4.8	0.89	4.3	96.36
	1×10^{-3}	0.12	897.0	4.1	0.90	3.06	98.02

by the adsorption of the organic molecules on the metal surface, decreasing the extent of the metal dissolution [35].

Adsorption isotherms

The action of an inhibitor in aggressive acid media is assumed to be due to its adsorption at the metal/solution interface. The adsorption of an organic adsorbate at a metal/solution interface can be regarded as a substitution adsorption process between the organic molecule in the aqueous solution $Org_{(sol)}$ and the water molecules on the metallic surface $H_2O_{(ads)}$ [36]:

$$Org_{(sol)} + xH_2O_{(ads)} \rightleftarrows Org_{(ads)} + xH_2O_{(sol)}. \quad (8)$$

Here x is the size ratio representing the number of water molecules replaced by a molecule of organic adsorbate. For organic inhibitors that have the ability to adsorb strongly on metal surface, thus impeding the dissolution reaction, the surface coverage (θ) can be evaluated as the IE The relationship between the IE and the bulk concentration of the inhibitor at constant temperature, which is known as isotherm, gives an insight into the adsorption process.

The most frequently used adsorption isotherms are Langmuir, Temkin, and Frumkin. So several adsorption isotherms were tested for the description of adsorption behavior of the studied compounds, and it is found that adsorption of Schiff bases on mild steel surface in HCl solution follows the Langmuir adsorption isotherm given by the following equations [37]:

$$\frac{C_{inh}}{\theta} = C_{inh} + \frac{1}{K_{ads}}, \quad (9)$$

$$K_{ads} = \frac{1}{55.5}\exp\left(-\frac{\Delta G_{ads}}{RT}\right), \quad (10)$$

where C_{inh} is the inhibitor concentration, θ is the fraction of the surface covered, K_{ads} is the equilibrium constant of the adsorption process, and ΔG_{ads} is the standard free energy of adsorption.

Figure 7 shows the dependence of the fraction of the surface covered C/θ as a function of the concentration (C) of Schiff bases.

It should be explained that other adsorption isotherms (Frumkin and Temkin) were checked and Langmuir adsorption isotherm is the best approximate between them. This is why the assumption is true for Langmuir adsorption isotherm.

The obtained plots of the inhibitors is linear with correlation coefficient higher than 0.99. The intercept permits the calculation of the equilibrium constant K_{ads} which are 166666.7 and 333333.3 M^{-1} for compounds 1 and 2, respectively. The values of K_{ads}, which indicate the binding power of the inhibitor to the steel surface, can lead to

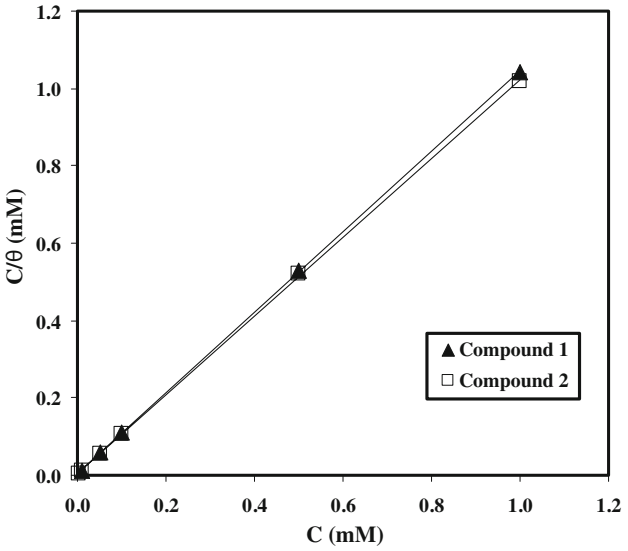

Fig. 7 Langmuir plots for compounds 1 and 2 on mild steel in 15% HCl

calculate the adsorption energy. Values of $\Delta G_{ads} = -39.74$ and -41.457 kJ mol^{-1} for compounds 1 and 2, respectively. The negative value of ΔG_{ads} means that the adsorption of Schiff bases on mild steel surface is a spontaneous process, and furthermore the negative values of ΔG_{ads} also show the strong interaction of the inhibitor molecule onto the mild steel surface [38, 39].

In general, values of ΔG_{ads} by -20 kJ/mol are compatible with the electrostatic interaction between the charged molecules and the charged metal. Those are more negative than -40 kJ/mol entail charge sharing or charge transfer from the inhibitor molecules to the metal surface [40]. The calculated ΔG_{ads} value, being closer to -40 kJ/mol, is between the threshold values for physical adsorption and chemical adsorption, it indicates that adsorption of Schiff bases on mild steel surface involves two types of interaction.

Effect of temperature

In order to calculate the activation energy of the corrosion process and investigate the mechanism of inhibition, potentiodynamic polarization measurements were performed in the temperature range of 35 to 65 °C in the absence and presence of 1×10^{-3} inhibitors. The obtained corrosion parameters are given in Table 5 and show when temperature increases, in the absence and presence of inhibitor, the I_{corr} increases.

The dependence of the corrosion current on temperature can be expressed by the Arrhenius equation:

$$I_{corr} = A\exp\left(\frac{-E_a}{RT}\right), \quad (11)$$

Table 5 Polarization parameters and corresponding IE for the corrosion of the mild steel in 15% HCl without and with addition of 1×10^{-3} M of Schiff bases at different temperatures

Inhibitor	Temperature (°C)	$-E_{corr}$ (mV)	I_{corr} (μA cm^{-2})	$-b_c$ (mV dec^{-1})	b_a (mV dec^{-1})	IE (%)
Blank	35	422	3985	123	91	–
	45	402	8030	111	89	–
	55	403	11160	110	85	–
	65	409	28300	105	83	–
Compound 1	35	420	191.2	152	98	95.2
	45	423	497.8	169	110	93.8
	55	416	848.1	119	129	92.4
	65	408	2462.1	131	136	91.3
Compound 2	35	403	53.2	169	115	98.7
	45	406	98.9	226	128	98.8
	55	405	178.2	198	134	98.4
	65	401	360.2	151	149	98.7

where I_{corr} is corrosion current, A is a constant, E_a is the activation energy of the metal dissolution reaction, R is the gas constant, and T is the temperature. The E_a values were calculated from the Arrhenius plots (Fig. 8) and the results are shown in Table 6.

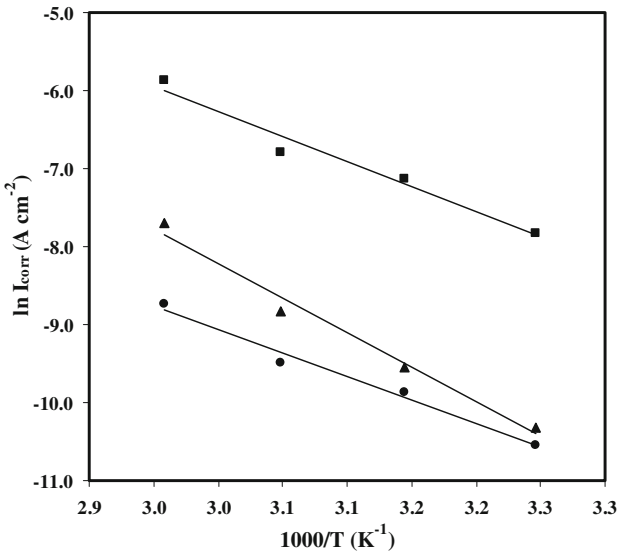

Fig. 8 Plotting ln (I_{corr}) vs. $1/T$ to calculate the activation energy of corrosion process in the presence of inhibitors: blank (*filled square*), compound 1 (*filled triangle*), and compound 2 (*filled circle*)

Table 6 Activation parameters of dissolution reaction of mild steel in 15% HCl solution containing 1×10^{-3} M concentrations of studied Schiff bases

Inhibitor	E_a (kJ mol^{-1})	ΔH^* (kJ mol^{-1})	ΔS^* (J mol^{-1} K^{-1})
Blank	53.6	50.91	−125.98
Compound 1	72.86	70.18	−95.79
Compound 2	54.63	51.95	−158.57

Radovici [41] classifies the inhibitors into three groups according to the temperature effects:

1. Inhibitors whose IE decreases with temperature increase. The value of the apparent activation energy, E_a, found is greater than that in the uninhibited solution.
2. Inhibitors whose IE does not change with temperature variation. The apparent activation energy does not change with the presence or absence inhibitors.
3. Inhibitors in whose presence the IE increases with temperature increase while the value of E_a for the corrosion process is smaller than that obtained in the uninhibited solution.

Unchanged or lower values of E_a in inhibited systems compared to the blank has been reported [42] to be indicative of chemisorption mechanism, whereas higher values of E_a suggest a physical adsorption mechanism.

The decrease in IE value with temperature increase and the higher value of E_a in presence of compound 1 can be interpreted as an indication for a physical or coulombic type of adsorption [43]. The higher E_a value in the inhibited solution can be correlated with the increased thickness of the double layer, which enhances the activation energy of the corrosion process.

IE of compound 2 does not change with temperature variation, and activation energy in the presence of inhibitor is close to that obtained for 15% HCl. This result probably was attributed to chemisorption of compound 2 on the steel surface [44].

An alternative formulation of Arrhenius equation is:

$$I_{corr} = \frac{RT}{N_A h} \exp\left(\frac{\Delta S^*}{R}\right) \exp\left(-\frac{\Delta H^*}{RT}\right), \quad (12)$$

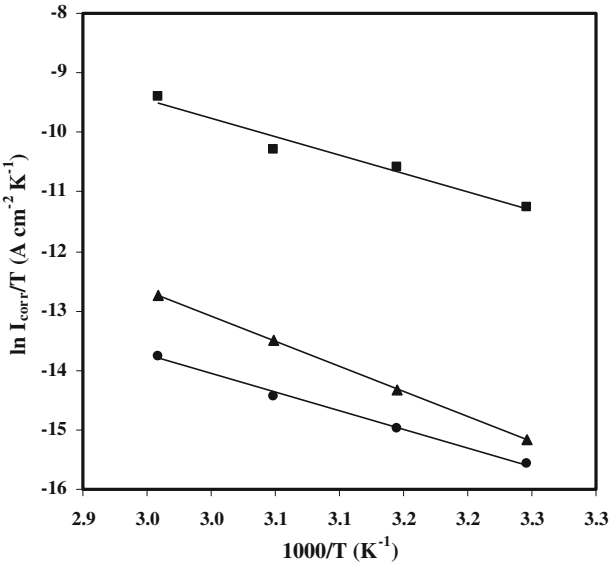

Fig. 9 Arrhenius plots of ln (I_{corr}/T) vs. $1/T$ in the absence and presence of 10^{-3} M Schiff bases: blank (*filled square*), compound 1 (*filled triangle*), and compound 2 (*filled circle*)

where h is Planck's constant, N_A is the Avogadro's number, R is the universal gas constant, ΔH^* is the enthalpy of the activation, and ΔS^* is the entropy of activation. Figure 9 shows a plot of ln (I/T) against $1/T$. Straight lines are obtained with a slope of $(-\Delta H^*/R)$ and an intercept of $(\ln(R/N_A h) + (\Delta S^*/R))$ from which the values of ΔH^* and ΔS^* are calculated and listed in Table 6.

The positive signs of ΔH^* reflect the endothermic nature of the mild steel dissolution process. The entropy of activation ΔS^* in the absence and presence of the inhibitors are large and negative. This indicates that the activated complex in the rate determining step represents an association rather than a dissociation step, meaning that a decrease in disordering takes place on going from reactants to the activated complex [45].

SEM investigation

The SEM images are taken and observed in order to support our findings. The SEM images of mild steel after immersion in 15% HCl for 24 h in absence and presence of 1×10^{-3} M of inhibitors 1 and 2 were performed and shown in Fig. 10a–c. Figure 10a shows that the mild steel surface was strongly damaged in HCl in the absence of inhibitors. As can be seen from Fig. 10b and c, there was much less damage on the surface of the mild steel with compounds 1 and 2.

Molecular structure effect

The mechanism of the inhibition processes of the corrosion inhibitors under consideration is mainly the adsorption one.

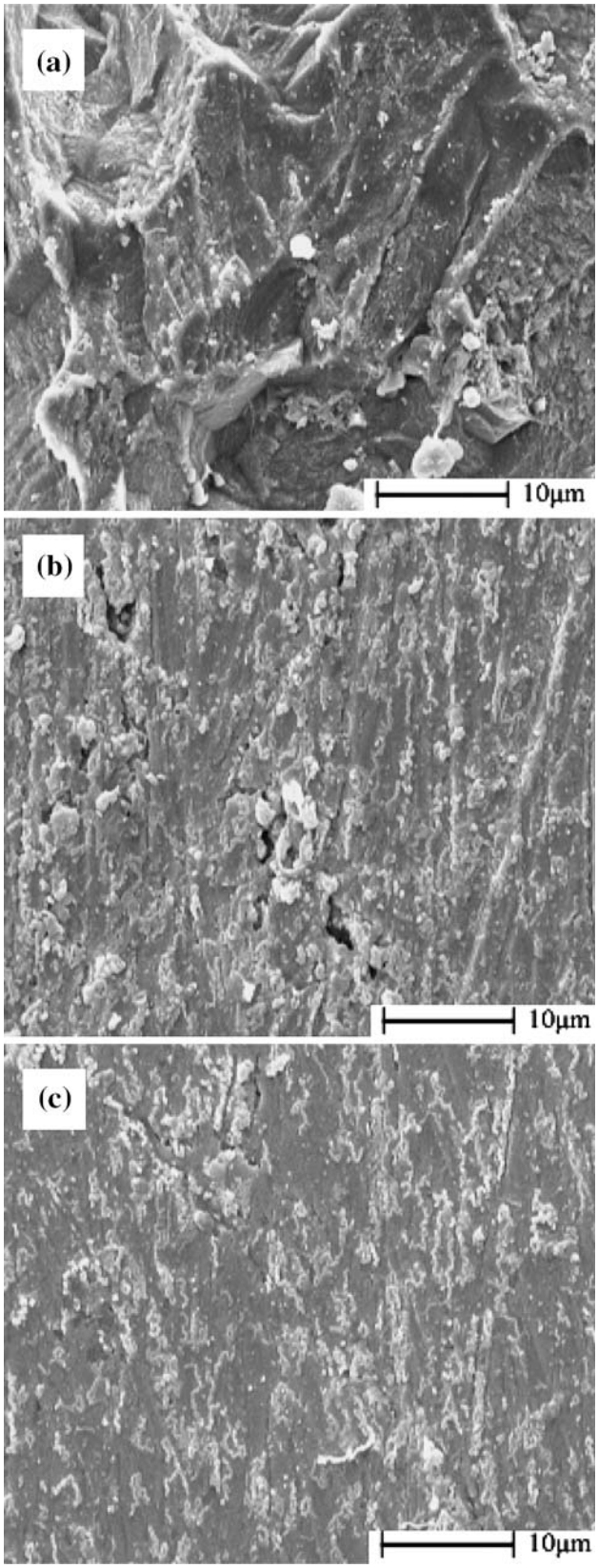

Fig. 10 The SEM mild steel specimens: **a** 15% HCl in the absence of Schiff base; **b** 15% HCl containing 10^{-3} M compound 1, and **c** 15% HCl containing 10^{-3} M compound 2

The process of adsorption is governed by different parameters that depend almost on the chemical structure of these inhibitors. Efficient adsorption is the result of π electrons of the aromatic system, double bonds, and electronegative nitrogen and sulphur atoms present in the structure.

The difference in the protection action of two Schiff bases can be attributed to the presence of different substituents to azomethine (–C=N–) group. The difference in IE between compounds 1 and 2 arises due to the presence of phenyl ring in compound 2 instead of presence of methyl group in compound 1 as substituent. Presence of phenyl ring in compound 2 causes that molecule of compound 2 has bigger conjugate π bonds among the aromatic rings than that of compound 1, so it gives higher IE. Other point of view for the difference in IE of two inhibitors lies in the size of the organic compound. As compound 2 is larger than compound 1, more effective adsorption and subsequently higher IE is true for it.

Conclusions

1. The both studied Schiff bases are excellent inhibitors and act as the mixed type inhibitors for mild steel corrosion in hydrochloric acid solution.
2. The results obtained from weight loss test and electrochemical measurements show that the inhibiting properties increase with inhibitor concentration. The IE increases in accordance to the order: compound 2 > compound 1 for all methods employed with small differences in their numerical values.
3. Double layer capacitances decrease with respect to blank solution when the Schiff base added. This fact may be explained by adsorption of Schiff base molecules on the mild steel surface.
4. The adsorption of Schiff bases on mild steel in 15% HCl solution follows Langmuir adsorption isotherm.
5. The thermodynamic parameters (K_{ads}, ΔG_{ads}) of adsorption for the studied compounds are calculated from their adsorption isotherms. The negative values of ΔG_{ads} show the spontaneity of the adsorption.
6. Activation parameters (E_a, ΔH^*, ΔS^*) for the corrosion of mild steel in 15% HCl were calculated. In the case of compound 1, activation energy increases with the addition of inhibitor, whereas activation energy of compound 2 is similar to that obtained in the absence of inhibitor. The increase in the activation energy in the presence of compound 1 may be attributed to the physisorption of molecules of this inhibitor on the mild steel, whereas the chemisorption mode is more probable for compound 2.
7. The SEM micrographs confirm the protection of the mild steel corrosion in 15% HCl solution by the Schiff bases studied.

Acknowledgement The authors gratefully acknowledge the Kashan University for the support of this research.

References

1. Wang CY, Wu GH, Zhang Q, Jiang LT (2008) J Mater Sci 43:3327. doi:10.1007/s10853-008-2506-4
2. Shibli SMA, Manu R (2008) J Mater Sci 43:4282. doi:10.1007/s10853-008-2622-1
3. Batory D, Blaszczyk T, Clapa M, Mitura S (2008) J Mater Sci 43:3385. doi:10.1007/s10853-007-2393-0
4. Xia SA, Zhou BX, Chen WJ (2008) J Mater Sci 43:2990. doi:10.1007/s10853-007-2164-y
5. Alyousif OM, Engelberg DL, Marrow TJ (2008) J Mater Sci 43:1270. doi:10.1007/s10853-007-2252-z
6. Moura V, Kina AY, Tavares SSM, Lima LD, Mainier FB (2008) J Mater Sci 43:536. doi:10.1007/s10853-007-1785-5
7. Geng HM, Wu XC, Wang HB, Min YG (2008) J Mater Sci 43:83. doi:10.1007/s10853-007-2084-x
8. Zhang D, Gao L, Zhou G (2008) J Appl Electrochem 38:71
9. Ramesh S, Rajeswari S (2004) Electrochim Acta 49:2701
10. Noor EA (2005) Corros Sci 47:33
11. Gopi D, Govindaraju KM, Manimozhi S, Ramesh S, Rajeswari S (2007) J Appl Electrochem 37:681
12. Refaey SAM, Taha F, Abdel-malak AM (2004) Appl Surf Sci 236:175
13. Mahmoud SS (2007) J Mater Sci 42:989. doi:10.1007/s10853-006-1389-5
14. Yurt A, Balaban A, Kandemir SU, Bereket G, Erc B (2004) Mater Chem Phys 85:420
15. Abdel-Maksoud SA (2004) Electrochim Acta 49:4205
16. Quraishi MA, Sardar R, Jamal D (2001) Mater Chem Phys 71:309
17. Wang HL, Liu RB, Xin J (2004) Corros Sci 46:2455
18. Quan Z, Chen S, Li Y, Cui X (2002) Corros Sci 44:703
19. Li S, Wang YG, Chen SH, Yu R, Lei SB, Ma H, Liu D (1999) Corros Sci 41:1769
20. Behpour M, Ghoreishi SM, Salavati-Niasari M, Ebrahimi B (2008) Mater Chem Phys 107:153
21. Aytac A, Ozmen U, Kabasakaloglu M (2005) Mater Chem Phys 89:176
22. Agrawal YK, Talati JD, Shah MD, Desai MN, Shah NK (2004) Corros Sci 46:633
23. Emregul KC, Atakol O (2004) Mater Chem Phys 83:373
24. Ita BI, Offiong OE (1999) Mater Chem Phys 59:179
25. Emregul KC, Kurtaran R, Atacol O (2003) Corros Sci 45:2803
26. Hosseini M, Mertens SFL, Ghorbani M, Arshadi MR (2003) Mater Chem Phys 78:800
27. Behpour M, Ghoreishi SM, Soltani N, Salavati-Niasari M, Hamadanian M, Gandomi A (2008) Corros Sci 50:2172
28. Ashassi-Sorkhabi H, Shaabani B, Seifzadeh D (2005) Appl Surf Sci 239:154
29. Ganjalli MR, Emami M, Rezapour M, Shamsipour M, Maddah B, Salavati-Niasari M, Hosseini M, Talebpour Z (2003) Anal Chim Acta 495:51
30. Quartarone G, Bonaldo L, Tortato C (2006) Appl Surf Sci 252:8251
31. Tamil Selvi S, Raman V, Rajendran N (2003) J Appl Electrochem 33:1175

32. Chauhan LR, Gunasekaran G (2007) Corros Sci 49:1143
33. Tavakoli H, Shahrabi T, Hosseini MG (2008) Mater Chem Phys 109:281
34. Hsu CH, Mansfeld F (2001) Corrosion 57:747
35. Benabdellah M, Touzani R, Aouniti A, Dafali A, El Kadiri S, Hammoutia B, Benkaddour M (2007) Mater Chem Phys 105:373
36. Morad MS, Sarhan AAO (2008) Corros Sci 50:744
37. Machnikova E, Whitmire KH, Hackerman N (2008) Electrochim Acta 53:6024
38. Yurt A, Bereket G, Kivrak A, Balaban A, Erk B (2005) J Appl Electrochem 35:1025
39. Quraishi MA, Rawat J, Ajmal M (2000) J Appl Electrochem 30:745
40. Ramesh Saliyan V, Adhikari AV (2008) Corros Sci 50:55
41. Radovici O (1965) Proceedings of the 2nd European symposium on corrosion inhibitors. Ferrara
42. Morad MS, Kamal El-Dean AM (2006) Corros Sci 48:3398
43. Quraishi MA, Jamal D (2003) Mater Chem Phys 78:608
44. Bentiss F, Traisnel M, Chaibi N, Mernari B, Vezin H, Lagrenée M (2002) Corros Sci 44:2271
45. Quraishi MA, Khan S (2006) J Appl Electrochem 36:539